Detection Efficiencies for InP, InAlAs, and InAlAs-InP Single-Photon Avalanche Photodiodes

David A. Ramirez, Majeed M. Hayat, *Senior Member, IEEE,* **Gauri Karve, Joe C. Campbell,** *Fellow, IEEE,* **Sergio N. Torres, Bahaa E. A. Saleh,** *Fellow, IEEE,* **and Malvin C. Teich,** *Fellow, IEEE*

Single-photon avalanche photodiodes (SPADs) are important devices for many visible-light to near-infrared applications that demand high single-photon detection efficiencies. These applications include satellite laser ranging, deep-space laser communication, time-resolved photon counting, quantum key distribution, quantum imaging, and quantum cryptography [1,2]. The performance of SPADs is usually assessed by the single-photon quantum efficiency (SPQE), also known as detection efficiency. This metric is a composite of the probability of detecting individual photons and the probability of false counts, which are due to dark carriers. Compared to the visible and shorter near-infrared wavelengths, the performance of III-V–based SPADs for applications in the 1.3–1.55 μm range remains relatively poor (e.g., SPQE is below 10% at 1.55 μm [3]). This is despite the remarkable advances in developing low-noise avalanche photodiodes (APDs) for linear-mode operation in the same wavelength range. These include APDs with thin multiplication regions (MR) as well as impact-ionization-engineered (I^2E) APDs [4]. In fact, there has been evidence that while thin APDs result in reduced excess noise factors, their breakdown characteristics may not be ideal for Geiger-mode operation [5]. This is primarily due to two factors: (1) Thin MRs require higher breakdown electric fields, which result in higher tunneling current and hence higher dark-count rates [6]; and (2) the transition from linear mode to Geiger mode, as a function of the excess bias, occurs more gradually in thin multiplication layers [5]. The latter behavior deviates the SPAD away from the ideal bimodal behavior (i.e., linear vs. Geiger mode) that is most desirable for single-photon detection.

In this paper we report theoretical results on the dependence of the SPQE on the type of material of the MR as well as its structure and width. We consider SPADs with hole-injection InP MRs, electron-injection $In_{0.52}Al_{0.48}As$ MRs, and hole-injection $In_{0.52}Al_{0.48}As$-InP heterojunction I^2E MRs. The model uses generalized breakdown probabilities based on the hard-threshold dead-space multiplication theory [7]. The main mechanism for dark-carrier generation considered in this paper is tunneling current, which dominates other sources of dark carriers at the high electric fields beyond breakdown [8].

Assuming that an optical pulse is present and at least one photon impinges on the SPAD, the SPQE is defined as the probability that a photon triggers an avalanche breakdown while no dark carrier triggers a breakdown. Mathematically, it is defined as $SPQE = (1 - P_d)P_{opt}/p_o$ [9], where P_d is the dark-count probability defined as the probability that at least one dark carrier (distributed at a random location in the MR) successfully triggers an avalanche breakdown, P_{opt} is the probability that at least one photon triggers an avalanche breakdown, and p_o is the probability that at least one photon impinges on the SPAD during the detection time.

Figure 1 shows the calculated SPQEs, as a function of the excess voltage, for SPADs with InP MRs of various widths. We assume a 2-ns on-pulse with repetition rate of 500 kHz [8]. Moreover, the average number of photons per pulse is assumed as $N_o = 0.1$ photons. Finally, the quantum efficiency of the SPAD is assumed as $\eta = 0.5$ at $\lambda = 1.55$ μm [10]. It can be seen that the peak SPQE decreases as the MR's width is reduced. This behavior is essentially due to the increase in the breakdown electric field in thin MRs, which results in an increase in the tunneling current. The latter results in an increase in the dark-count probability causing the SPQE to decrease. Additionally, as the width of the MR increases the SPQE versus excess-voltage curve becomes wider, this is measured by the full-width-half-maximum (FWHM). A large FWHM implies less variability, with respect to fluctuations in the applied voltage, in the SPQE about its peak. Thus, thicker devices offer less sensitivity to voltage variation.

Our calculations show that the heterojunction MRs have an added property. Just as impact-ionization engineering of the MR causes a reduction in the excess noise factor, it can have a beneficial effect on the SPQE. The curves in Fig. 2 depict the calculated SPQEs for $In_{0.52}Al_{0.48}As$, InP, and a specific $In_{0.52}Al_{0.48}As$-InP heterojunction MR; the MRs' width is 200 nm in all cases. The results indicate that for thin MRs, the $In_{0.52}Al_{0.48}As$-InP heterojunction outperforms both $In_{0.52}Al_{0.48}As$ and InP MRs. However, as the width of the MR-width increases, the performance advantage of the $In_{0.52}Al_{0.48}As$-InP MR becomes less significant and eventually approaches that of the InP MR. This is essentially due to the diminishing effect of dead space in thick MRs. We emphasize that the SPQE of the heterojunction is sensitive to the widths of the individual layers of the heterojunction, which are in this example 30 nm and 170 nm for the $In_{0.52}Al_{0.48}As$ and InP layers, respectively.

In general, for a given $In_{0.52}Al_{0.48}As$-InP heterojunction, there is an optimal combination of the widths of the individual layers that maximizes the SPQE. It was found that the optimal width of the buildup layer is slightly less than the hole dead space of $In_{0.52}Al_{0.48}As$, calculated at the breakdown field. For example, for the widths of 150 nm, 200 nm, and 300 nm, the hole dead spaces are found to be 29.9 nm, 30.2 nm, and 32.1 nm, respectively. On the other hand, our peak-SPQE-based optimization of the same family of structures yields $In_{0.52}Al_{0.48}As$ widths of 30 nm, 30 nm, and 32 nm, which approximate the hole dead space at peak SPQE for the various widths considered.

Finally, motivated by the new emerging communication applications [1], we have investigated the SPAD's performance by considering the channel capacity of a single-photon-based receiver. The optimization, in terms of the structure and width of the MR, showed similar trends compared to that of the SPQE. However, the optimal operating point for one metric gives a poor performance when used to optimize the other. For example, the applied voltage at which the SPQE peaks ($V = 20.5$ V) is different from that at which channel capacity peaks ($V = 19$ V). If the channel-capacity-optimized heterostructure SPAD is operated at $V = 20.5$ V, the channel capacity would be 58% below its maximum value (at $V = 19$ V).

In conclusion, our analytical modeling confirms that reducing the thickness of the MR has a detrimental effect on Geiger-mode operation of a SPAD. On the other hand, in heterojunction MRs, including a high-bandgap $In_{0.52}Al_{0.48}As$ layer before the InP layer can improve the SPQE. This effect is akin to the noise reduction observed in I^2E heterojunction APDs operated in the linear mode. Also, device optimization must be performed with the application (sensing vs. communication) in mind.

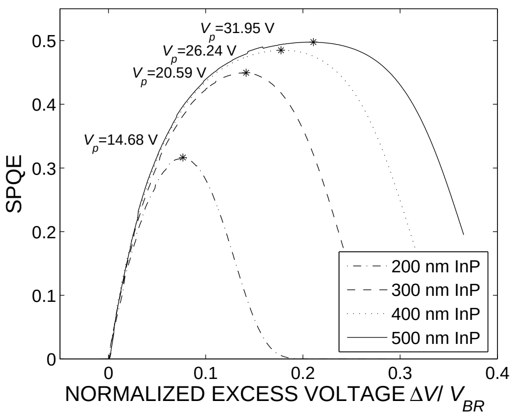

Figure 1: Calculated SPQE as a function of the normalized excess voltage for each width. The reverse-bias voltage corresponding to the peak SPQE is also shown for each width.

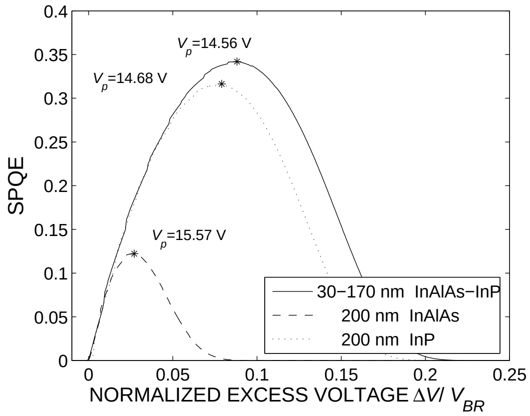

Figure 2: Calculated SPQE for 200-nm InP (dotted) and 200-nm (dashed) $In_{0.52}Al_{0.48}As$ MRs, and a 30-nm–170-nm $In_{0.52}Al_{0.48}As$-InP heterojunction MR (solid).

References

[1] A. Biswas *et al.*, *2004 IEEE/LEOS Ann. Meeting*, pp. 74–75, 2004.
[2] A. Spinelli *et al.*, *Rev. Sci. Instrum.*, vol. 67, pp. 55–61, 1996.
[3] G. Ribordy *et al.*, *J. Modern Optics*, vol. 51, pp. 1381-1398, 2004.
[4] N. Li *et al.*, *Appl. Phys. Lett.*, vol. 82, pp. 2175–2177, 2003.
[5] J. S. Ng *et al*, *2003 IEEE/LEOS Ann. Meeting*, vol. 2, pp. 773–774, 2003.
[6] M. A. Saleh *et al*, *Appl. Phys. Lett.*, vol. 79, pp. 4037–4039, 2001.
[7] M. M. Hayat *et al.*, *IEEE J. Quantum Electron.*, vol. 39, pp. 179–185, 2003.
[8] G. Karve *et al.*, *Appl. Phys. Lett.*, vol. 86, 63505–1–3, 2005.
[9] Y. Kang *et al.*, *Appl. Phys. Lett.*, vol. 83, pp. 2955–2957, 2003.
[10] G. Karve *et al.*, *IEEE J. Quantum Electron.*, vol. 39, pp. 1281–1286, 2003.